GO BEYOND
Pioneers of omics webinar series

View recent webinar recordings about exciting work at the forefront of omics research:

Artificial intelligence in proteomics

Presenters: Mathias Wilhelm, Martin Frejno, Karl Mechtler

Cancer research – towards personalized medicine

Presenters: Tami Geiger, Nicholas Rattray, Julio Sampaio

Biomarker discovery and validation of biological fluids

Presenters: Roland Bruderer, Chloé Jacquemin, Ivalya Roberts, Santosh D. Bhosale

Metabolomics approaches for systems biology

Presenters: Gunda Koellensperger, Evelyne Rampler, Cristina Coman,

Marina Wright Meulas, Tito Damiani

A new nano UHPLC for omics and biopharma (sessions in English and German)

Presenters: Nicola Berner, Karl Mechtler, Alexander Boychenko

Interactomics/Spatial omics

Presenters: Theodore Alexandrov, Manuel Matzinger, Alexey Chernobrovkin,

Alessandro Ori, Eneko Villanuev

Participation is free of charge. Sign-up now to view on-demand.
2022 sessions will be announced soon.

Learn more

thermo scientific

Effects of oxygen plasma ashing treatment on carbonate clumped isotopes

Qi Adlan | Amelia J. Davies | Cédric M. John

Department of Earth Science and Engineering, Imperial College London, London, UK

Correspondence
Q. Adlan, Department of Earth Science and Engineering, Imperial College London, London SW7 2AZ, UK.
Email: q.adlan17@imperial.ac.uk

Funding information
Indonesia Endowment Fund for Education (LPDP Scholarship)

Rationale: For clumped isotope analysis (Δ_{47}), hydrocarbon and organic molecules present an important contaminant that cannot always be removed by CO_2 purification through a Porapak-Q trap. Low-temperature oxygen plasma ashing (OPA) is a quick and easy approach for treatment; however, the impact of this treatment on the original carbonate clumped isotope values has never been fully studied.

Methods: We tested the isotopic impact of OPA using three natural samples with a large range of initial Δ_{47} values. Crushed and sieved (125 µm mesh) samples were placed into a Henniker Plasma HPT-100 plasma system and treated at a flow rate of 46 mL/min and a power of 100 W at a vacuum of 0.2 mbar for 10, 20, 30 and 60 min before clumped isotope analysis using two MAT 253 isotope ratio mass spectrometers modified to measure masses 44–49.

Results: OPA treatment for 30 min or more on calcite powder samples has the potential to alter the clumped isotopic composition of the samples beyond analytical error. A systematic positive offset is observed in all samples. The magnitude of this alteration translates to a temperature offset from known values ranging from 4°C to 13°C. We postulate that the observed positive offset in Δ_{47} occurs because the bonds within lighter isotopologues are preferentially broken by plasma treatment, leading to an artificial increase in the 'clumping' value of the sample.

Conclusions: We recommend that any laboratory performing OPA treatments should reduce the runs to 10–20 min or carry out successive runs of 10 min followed by sample stirring, as this procedure showed no alteration in the initial Δ_{47} values. Our results validate the use of OPA for clumped isotope applications and will allow future research to use clumped isotopes for challenging samples such as oil-stained carbonates, bituminous shales or host rocks with very high organic carbon content.

1 | INTRODUCTION

Since the introduction of carbonate clumped isotope thermometry more than a decade ago, the number of laboratories, as well as the number of geoscience applications using this technique, has increased rapidly. The naturally occurring, multiply substituted isotopologues (clumped isotopes) of ^{13}C and ^{18}O are ideal for paleotemperature reconstruction because no information on the oxygen isotope composition of the water is required.[1] Carbonate clumped isotopes have wide applications such as reconstructing burial history,[2–10] carbonate diagenesis,[11–14] constraining the conditions for dolomitization,[15–18] reconstructing subsurface fluid flow,[19–21] estimating the burial pressure regime of carbonates,[22] reconstructing past glacial/interglacial temperature variations,[23,24] constraining the

uplift rates on continents,[25] and estimating fault-related temperature and fluid composition.[26]

As carbonates are widespread minerals found in sedimentary basins and crystalline rock complexes, further applications of this technique can provide important information on conditions for economic mineral deposits[27,28] and characterization of hydrocarbon reservoirs.[29,30] A wide range of applications implies a wide range of sample types used for clumped isotopes, and therefore it has become increasingly more important to evaluate possible sources of uncertainties related to sample contamination. The most common problem in stable isotopic measurements, other than the presence of water, is the presence of hydrocarbon (eg, bitumen) and adhering organic material, which can affect the measurements of both carbonate clumped isotopes[30,31] and conventional bulk isotopes.[32–34] These organic components react with phosphoric acid (H_3PO_4) during acid digestion to generate molecular gaseous species that have similar molecular weights to the carbon dioxide molecules. These radicals and ions in the 44–46 mass range (eg, NO_2) produce isobaric effects that interfere with the mass spectrometric determination of $\delta^{13}C$ and $\delta^{18}O$ values. Molecular species such as $^{32}S^{16}O$ that have similar masses to mass 48 and 49 of CO_2[35] (or also $^{15}N^{16}O_2$, $^{15}N^{14}N^{18}O$, $^{14}N^{15}N^{18}O$, CH_2Cl_2, C_5H_{12}, CCl^+ produced from CH_3Cl or CH_2Cl_2[36]) lead to isobaric interferences with the mass 47 of CO_2. For masses in the m/z 47–49 range, these effects are several orders of magnitude more important due to the low abundance of the corresponding naturally occurring isotopologues, and this significantly impacts clumped isotope measurements.[31]

In the field of conventional bulk isotope analysis, it has become common practice to perform a treatment to remove organic matter.[32,37–44] Low-temperature oxygen plasma ashing (OPA) is widely used to remove organic matter from samples using ionized oxygen[38,45] with a working temperature of 60°C–70°C.[46] The effect of low-temperature OPA treatment on the initial bulk isotopic composition has been demonstrated as being neglectable or within the limit of analytical error.[44] A recent study, however, indicated that low-temperature OPA treatment produced a maximum change of the initial bulk isotopic ratio of +0.30‰ for $\delta^{13}C$ values and −0.12‰ for $\delta^{18}O$ values for a 2–6 h 125°C treatment.[33]

For carbonate clumped isotope measurements, cleaning of CO_2 from volatile organic contaminants generated by acid digestion is achieved through a static Porapak-Q trap held under vacuum at temperatures below 0°C.[31,35] However, there are some indications that the Porapak-Q trap is not sufficient to clean samples with abundant organic radicals during the purification process. Although it was not discussed in detail in previous publications, raw data from a previous clumped isotope study[30] performed in our laboratory showed that contamination issues could radically be reduced by using OPA treatment on organic-rich samples, as indicated by lower Δ_{48} offsets and 49 parameters after OPA treatment. However, to date, no study has systematically investigated potential fractionation effects that low-temperature OPA could have on the initial Δ_{47} values of carbonates. For instance, in the previously cited study,[30] a Δ_{47} lowering of 0.011‰–0.040‰ was observed and attributed to the OPA-treated samples being free of contaminants (contamination results in positive isobaric effects on mass 47), but it is also possible that the change was due to a secondary alteration of the initial Δ_{47} values.

Here, we present results of a study specifically designed to test whether OPA treatment has an impact on clumped isotope values. This is critical because clumped isotopes rely on high-resolution measurement, and even small offsets could significantly bias the temperatures derived from this technique.

2 | MATERIALS AND METHODS

2.1 | Samples

To test the effects of OPA treatment, we selected three natural samples with a large range of initial Δ_{47} values: an internal 'Oamaru limestone' (IOL) standard, a sample of vein calcite from Jabal Madar, Oman (JMF-6A) and our internal Carrara marble (ICM) standard. The IOL samples were previously documented as 'least cemented homogenous Oligocene limestones' and characterized by $\delta^{18}O$ and $\delta^{13}C$ values between 0‰ and 1‰ Pee Dee Belemnite (PDB) and 0‰ and 1.5‰ PDB, respectively.[47] The JMF-6A samples were previously documented as 'macro-columnar calcite' with $\delta^{18}O$ and $\delta^{13}C$ values between −16‰ and −12‰ Vienna Pee Dee Belemnite (VPDB) and −8‰ and −2‰ VPDB, respectively.[48]

Both IOL and ICM have been routinely measured as calcite standards on our instruments. The JMF-6A calcite sample was selected based on its isotopic homogeneity, and its Δ_{47} values lie between those of IOL and ICM. The samples were crushed with an agate mortar and pestle and then sieved through a 125 μm sieve. Fourier-transform infrared spectroscopy (Nicolet 5700 FT-IR spectrometer; Thermo Fisher Scientific, Waltham, MA, USA) was used to ensure that the samples were homogenous and to qualitatively estimate the mineralogy of JMF-6A and IOL. The Δ_{48} offset values of IOL and JMF-6A were, respectively, 0.044‰ and 0.038‰ on average, whereas the 49 parameters were, respectively, 0.177 and 0.131 on average. The choice of a wider range of Δ_{47} values was driven by the need to test whether the oxygen reagent-isotopic exchange impacted the carbonates and whether this effect was proportional to the clumped isotope composition of the sample. The Δ_{47} carbon dioxide equilibrated scale (CDES) values of IOL, JMF-6A and ICM were 0.732 ± 0.005‰ (n = 11), 0.629 ± 0.008‰ (n = 10) and 0.411 ± 0.003‰ (n = 21), respectively.

2.2 | Testing treatment times of 10, 20, 30 and 60 min with OPA

All powdered samples were weighed to 20 mg before being sprinkled evenly on a petri dish 60 mm in diameter with a side (wall height) of

15 mm to ensure a maximum surface area of the mineral exposed to the plasma treatment. The petri dish was placed into a Henniker Plasma HPT-100 chamber (100 mm diameter × 280 mm length; Henniker Scientific, Runcorn, UK) and treated with low-temperature plasma ashing under oxygen at a flow rate of 46 mL/min and a power of 100 W, with a vacuum condition of 0.2 mbar before gas flow and increasing to 2 ± 0.05 mbar during the treatment with gas in the chamber. The HPT-100 plasma chamber used in our study was the same instrument used previously to effectively remove organic contaminants within 5 min[30] and 40 min (2 × 15–20 min, with shaking and 5 min resting time between OPA treatments).[49] As a consequence, we tested OPA treatment times of 10, 20 and 30 min in our study to see if OPA impacted the Δ_{47} values, and potentially the $\delta^{18}O$ values, $\delta^{13}C$ values, Δ_{48} offsets and 49 parameters of our samples.

The instrument specification comparison shows that the power source used in the HPT-100 in our study was 50 W lower than that of the POLARON PT7160 (Quorum Technologies, Laughton, UK) used for the previous organic matter removal experiment.[38] The lower power of the HPT-100 generates a lower radio frequency (RF), which yields a lower oxidation potential[45] of O_2^+, O, O_2, O^-,[50] and electrons to react with the sample surface. Based on three temperature measurements, the working temperature inside the plasma chamber of our machine ranged between 65°C and 70°C after 30 min, 57°C and 60°C after 20 min, and 37°C and 43°C after 10 min. The temperature was measured on the petri dish surface using a wire probe-digital thermometer, 3–5 s after the plasma treatment; thus, the actual temperatures probably were slightly higher. This chamber temperature is lower than the 125°C reported for the plasma chamber in a similar bulk stable isotope cleaning experiment.[33] The lower chamber temperature is favourable as clumped isotopes are susceptible to reordering at elevated temperatures.[2,4] The actual plasma chamber temperature of the POLARON PT7160 used in the previous cleaning study[38] is unknown; however, the technical information suggests 10°C–35°C in 95% maximum humidity. This previous cleaning study[38] used a treatment duration of 300–1860 min before stable isotope measurement. The main part of our plasma experiment focuses on the detection of alteration using three different samples, whereas the secondary part focuses on the

best way to prevent alteration using only the ICM sample. The OPA experiment design in this study is shown in Figure 1.

2.3 | Stable isotope measurement

Measurements of clumped isotopes, $\delta^{18}O$ and $\delta^{13}C$, were carried out in the Qatar Stable Isotope Laboratory at Imperial College London using our fully automated prototype IBEX (Imperial Batch EXtraction) system. Samples of calcite powder (4 mg) were preloaded on a 40-position carousel, and each sample was individually dropped into a vacuum-sealed common acid bath for reaction with 105% orthophosphoric acid at 90°C for 10 min.[51,52] This acid digestion generates CO_2, which flows through a series of water traps, silver wool and a Porapak-Q trap[17,35,49] to remove water, sulphur and hydrocarbons. The resulting purified CO_2 was then automatically loaded and analysed using a dual inlet Thermo MAT 253 isotope ratio mass spectrometer (Thermo Instrument, Bremen, Germany) modified with Faraday collectors registered for m/z 44–49. The measurements were conducted using a reference gas CO_2 standard from High Purity gas (BOC, Barking, UK) with values of $\delta^{13}C$ VPDB −36.8‰ and $\delta^{18}O$ VSMOW 8.6‰.

Each replicate measurement comprises eight acquisitions with seven cycles each of 26 s integration time.[53] The measurement is repeated seven times per replicate in two different mass spectrometers (both MAT 253 instruments) with a total analysis time of 2 h per replicate on each mass spectrometer: 'Pinta' equipped with an automatic prototype IBEX line and 'Santa Maria' used with a manual line to prepare samples. In this study, we measured a minimum of nine replicates per sample for both IOL and JMF-6A samples and six replicates per sample for ICM, which yielded 127 measurements totalling 254 h of analysis time. To increase the throughput, 10% of the measurements were made by manual purification of CO_2 following a published procedure[13] and analysed on our second Thermo MAT 253 mass spectrometer. The manual line is similar in design to the IBEX but has no carrier gas, relying instead on cryogenic vacuum transfer. The analytical method (calculations of raw Δ_{47}, $\delta^{18}O$ and $\delta^{13}C$ values) of both systems (manual and IBEX) was similar.

FIGURE 1 Research design. The label 'Results 1, 2 and 3' refers to clumped isotope measurements of the untreated, 10 min, 20 min and 30 min oxygen plasma ashing (OPA) treatments, respectively, for the three samples. Result 4 refers to the experiment where the petri dish was taken out of the plasma chamber to stir the powders with less than 3 min breaks between 10 min plasma exposures [Color figure can be viewed at wileyonlinelibrary.com]
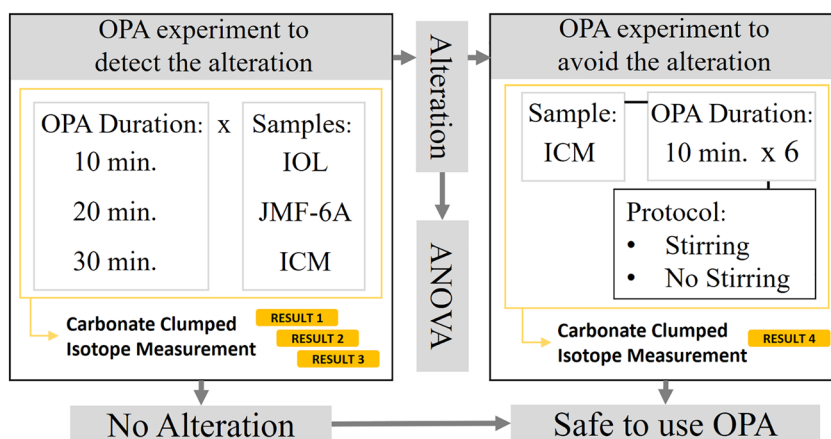
2.4 | Data analysis and reduction

Calculations and corrections of raw Δ_{47}, $\delta^{18}O$ and $\delta^{13}C$ values were performed using the free software Easotope.[53] For 10% of the samples prepared in the manual line, the first correction was for mass spectrometer non-linearity performed on the raw Δ_{47} values using a series of heated gases with different bulk isotopic compositions and carbonate standards.[35] For samples run on the IBEX, all the standards were carbonates, and we used a pressure baseline correction following the methods developed at the ETH Zürich.[54] Next, the Δ_{47} results were projected in the absolute reference frame or CDES[55] based on routinely measured ETH1, ETH2, ETH3, ETH4 and Carrara marble (ICM) carbonate standards.[49,56] The standard to samples ratio used in our study is 1:3. The last correction to the raw Δ_{47} values was to add an acid correction factor of 0.088‰ to obtain a final $\Delta_{47(CDES)}$ value.[57] The bulk $\delta^{18}O$ value was corrected for acid digestion at $90°C$ by multiplying the value by 1.0081 using the published fractionation factor.[58] Mass 48 and mass 49 signal spikes were used as indicators for the presence of hydrocarbons, chlorocarbons[35,36] and sulphur-bearing contaminants.[35,59] Contamination was monitored by observing the values on mass 48 and 49 from each measurement, using a Δ_{48} offset value < 1.5‰ and/or a 49 parameter value < 0.3 as a threshold to exclude individual replicates from the analysis.[31] To ensure that no bias in Δ_{47} offset was caused by using different purification lines and mass spectrometers, the results were compared both with and without the 10% data acquired with the manual purification line.

2.5 | Statistical methods

The clumped isotope Δ_{47}, $\delta^{18}O$ and $\delta^{13}C$ values of all samples (Carrara marble, IOL and JMF-6A) are normally distributed,[49] allowing for the application of parametric statistical tests on our sample data. Statistical analysis of one-way ANOVA (analysis of variance) was carried out using SPSS 25 software (IBM, Armonk, NY, USA). This statistical method was performed only on the IOL and JMF-6A samples. The null hypothesis was defined as plasma-treated samples representing the same population as the initial untreated sample. The alternative was that the mean results from our 10, 20 and 30 min OPA treatment are distinguishable as a unique population.

The power analysis[60] was implemented after the ANOVA test to quantify the likelihood that the null hypothesis could be rejected. For this analysis, the alpha level used was 0.05, whereas the effect size (partial eta-squared) was obtained from the ANOVA results.[60]

If the ANOVA test indicated no statistically significant difference among the population but that the mean value of results indicated a systematic offset for a given population, we then applied the least significant difference (LSD) T-test[61] to focus on relative differences between the four populations (initial, 10, 20 and 30 min OPA). This multiple comparison test (LSD) provides useful information even if the overall ANOVA results are not statistically significant. Although multiple comparison tests are commonly applied only after the null hypothesis of homogeneity is rejected, this practice is regarded as 'unfortunate common practice' by some statisticians.[62]

3 | RESULTS

The isotopic composition (Δ_{47}, $\delta^{18}O$ and $\delta^{13}C$ values) of all three samples treated with 10, 20, 30 and 60 min of OPA is shown in Table 1. Full details of the results can be found in the supporting information (Supplementary 1). Previous work[31,63] has shown that, due to the presence of the Porapak-Q trap in the purification line, the standard deviation of the $\delta^{18}O$ value of ICM was high (0.6‰[63] and 0.2‰[31]) at a trap temperature of $-35°C$. Given previous work on this topic, impacts on the bulk isotopic trends are not the focus of our study due to the high standard deviation. Instead, we focused on the Δ_{47} result.

3.1 | Δ_{47} alteration

The Δ_{47} results are presented as a box plot with 95% confidence level with the mean value shown by a red line (Figure 2) and one standard error (SE) representing uncertainty. In this section, the term 'value' is understood to mean the 'mean value' of the total number of replicate measurements for each standard or sample. The Δ_{47} value of IOL deviates by $-0.003‰$ from the control population after a 10 min plasma treatment and by $-0.002‰$ after a 20 min plasma treatment. For sample JMF-6A, the Δ_{47} deviated by $+0.004‰$ after the 10 min treatment and by $-0.005‰$ after the 20 min plasma treatment. All these results are within the analytical error (±1 SE) of 0.005‰ of the initial IOL value and within 0.008‰ of the initial JMF-6A value.

The 30 min OPA treatment of IOL resulted in a $+0.014‰$ deviations in the Δ_{47} value. This positive deviation of Δ_{47} occurred in 8 out of 10 measurements, and 50% of the measurements yielded a positive alteration within ~±3 SE of the initial IOL value. The same plasma duration for JMF-6A samples resulted in a $+0.024‰$ offset from the initial value. This positive offset occurred in eight out of nine measurements, and 55% of the total measurements show a positive alteration within ±3 SE of the initial JMF-6A value. For the ICM samples, the 30 min plasma treatment resulted in $+0.011‰$ deviations in the Δ_{47} value, within ±3 SE of the initial value. We compared the results including and excluding the 10% of manual line data, and there is no significant difference (less than 1 SE change in the average value). However, the systematic offset after 30 min of plasma treatment persisted.

One-way ANOVA tests showed that all the plasma treatment on IOL and JMF-6A had no significant impact ($\alpha = 0.05$) on the Δ_{47} parameter with $F(3,37) = 1.708$, $P = 0.182$ for IOL and $F(3,33) = 2.639$, $P = 0.066$ for JMF-6A (Table 2). Using our calculated effect size of 0.125 and 0.181, the power analysis[60] on IOL and JMF-6A

TABLE 1 Carbonate clumped isotope parameter (Δ_{47}) and bulk isotope composition ($\delta^{18}O$ and $\delta^{13}C$ values) of IOL, JMF-6A and ICM before (initial values) and after OPA pre-treatment

Sample ID	OPA treatment duration (min)	n	$\delta^{13}C$ (‰,VPDB)	$\delta^{13}C$ SE (‰)	$\delta^{18}O$ (‰,VPDB)	$\delta^{18}O$ SE (‰)	Δ_{47} (‰, CDES)	Δ_{47} SE (‰)	Δ_{47} offset[a] (‰)
Oamaru limestone, New Zealand									
Initial value	0	11	0.289	0.011	0.355	0.023	0.732	0.005	0
IOL10	10	10	0.281	0.020	0.386	0.024	0.729	0.007	−0.003
IOL20	20	10	0.303	0.010	0.348	0.018	0.729	0.006	−0.002
IOL30	30	10	0.327	0.012	0.410	0.037	0.746	0.007	0.014
Jabal Madar calcite vein, Oman									
Initial value	0	10	−7.895	0.024	−14.732	0.028	0.629	0.008	0
JMF10	10	9	−7.827	0.047	−14.733	0.096	0.633	0.006	0.004
JMF20	20	9	−7.910	0.022	−14.763	0.028	0.624	0.009	−0.005
JMF30	30	9	−7.812	0.041	−14.664	0.049	0.653	0.008	0.024
Carrara marble standard									
Initial value	0	21	2.060	0.006	−1.894	0.009	0.411	0.003	0
ICM10X3	10x3[b]	8	2.070	0.007	−1.898	0.021	0.401	0.005	−0.010
ICM30	30	7	2.059	0.015	−1.906	0.045	0.422	0.006	0.011
ICM10X6NS	10x6[c]	7	2.056	0.004	−1.879	0.044	0.413	0.003	0.002
ICM10X6S	10x6[d]	6	2.035	0.019	−1.947	0.047	0.407	0.004	−0.004

No systematic change in the Δ_{48} offset and 49 parameters was found.

CDES, carbon dioxide equilibrated scale; ICM, internal Carrara marble; IOL, internal Oamaru limestone; JMF-6A, Jabal Madar; OPA, oxygen plasma ashing.

[a]The mean value of the plasma-treated sample minus the untreated mean value.

[b]The total duration of OPA pre-treatment was 30 min; the treatment was ceased every 10 min to stir the sample powder.

[c]The total duration was 60 min; the treatment was ceased every 10 min with no stirring procedure introduced.

[d]The total duration was 60 min; the treatment was ceased and stirred every 10 min.

yielded a value of 0.0853 and 0.119 at the 0.05α value. These are considered as low values (<0.2),[60] implying that it is difficult to prove a statistical difference between the groups, even if a difference might exist. The size of the data set (n) plays an important role in this power analysis, as the power value has a positive correlation to the size of the data set.[64] Our ability to reject the null hypothesis would be improved with larger data sets (n).

Multiple comparison LSD tests on IOL and JMF-6A (Table 2) provide a numerical analysis that quantifies what we visually observe in the box plot, even if the overall ANOVA results are not statistically

FIGURE 2 Box plot result of oxygen plasma ashing treatment on internal Oamaru limestone (IOL), Jabal Madar (JMF-6A), internal Carrara marble (ICM) and ICM 60 min (Results 1, 2, 3 and 4). Mean value is shown by red lines [Color figure can be viewed at wileyonlinelibrary.com]
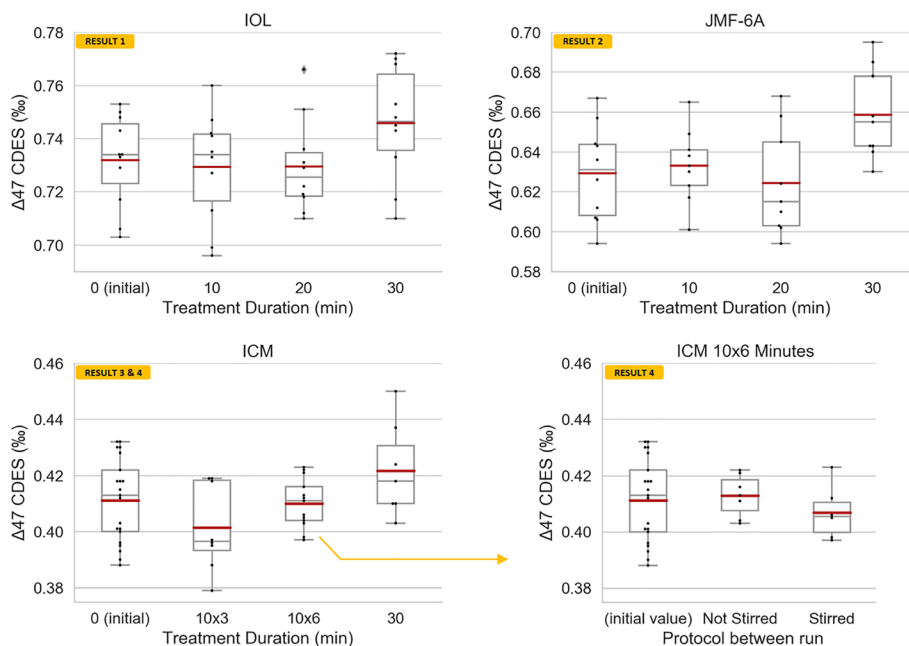
TABLE 2 ANOVA and post hoc LSD analysis of IOL and JMF-6A samples

ANOVA	Sum of squares	DF	F	P-value	Post hoc LSD		Mean difference	P-value	95% confidence level	
									Lower bound	Upper bound
IOL/Oamaru limestone										
Between group	0.002	3	1.708	0.182	Initial vs.	10 min	0.003	0.766	−0.015	0.020
Within group	0.014	37				20 min	0.002	0.775	−0.015	0.019
Total	0.016	40				30 min	−0.014	0.103	−0.031	0.003
JMF-6A/Jabal Madar calcite										
Between group	0.004	3	2.639	0.066	Initial vs.	10 min	−0.004	0.725	−0.026	0.018
Within group	0.018	33				20 min	0.005	0.653	−0.017	0.027
Total	0.022	36				30 min	−0.024	0.033	−0.046	−0.002

The null hypothesis was not rejected for all groups of treatment, but there is a noticeable difference between the mean value of the 30 min treatment and the initial value. The LSD post hoc reveals a distinguishable difference in the *P*-value on the 30 min plasma treatment.
ANOVA, analysis of variance; DF, degrees of freedom; IOL, internal Oamaru limestone; JMF-6A, Jabal Madar; LSD, least significant difference.

significant. From this LSD test, the *P*-value of the initial vs 30 min OPA data comparison for IOL is 0.103, which implies no statistical significance ($\alpha = 0.05$) between the two populations. However, the initial vs 10 min and the initial vs 20 min OPA data comparisons for IOL yield higher values of 0.766 and 0.775, respectively. For the JMF-6A, the *P*-value of the initial vs 30 min OPA data comparison reached 0.033, implying a statistical difference between the two populations. The initial vs 10 min and the initial vs 20 min OPA data comparisons for JMF-6A yield higher values of 0.725 and 0.653, respectively. The LSD results suggest that the populations of the 30 min OPA treatment are likely to be different from the initial condition, whereas this is not the case for the 10 min and 20 min OPA treatments.

3.2 | Testing variations of the OPA protocol on ICM

A variation of the OPA protocol (Table 1) was performed on ICM to observe the effect of the total exposure area to the plasma on the Δ_{47} value (Figure 2, Result 4). Three treatments of 10 min of OPA were performed sequentially on a sample, with stirring of the powder using a glass rod between the runs. This experiment resulted in a Δ_{47} offset of −0.010‰, that is, within ±3 SE of the untreated ICM sample. Furthermore, an experiment of six OPA treatments of 10 min each with no stirring yielded a Δ_{47} value within the analytical error (± 1 SE) of the untreated ICM sample, whereas the stirred samples yielded a Δ_{47} offset of −0.004‰, 1 ppm below the ±1 SE of the untreated ICM sample.

4 | DISCUSSION

4.1 | Contamination and effectiveness of the OPA treatment

The principle of the OPA method is that excited oxygen (O_2^+, O, O_2, O^-) and electrons are created by exposing oxygen reagent at a low temperature to radio frequencies in a vacuum chamber.[50] When these particles contact the sample surface, they oxidize organic particles into CO_2 and water vapour.[65]

Traditionally, two contamination indicators are used to screen data for clumped isotopes, the Δ_{48} offset and 49 parameters.[53] Replicate samples with values exceeding an acceptable threshold (1.5‰ for the Δ_{48} offset and 0.2 for the 49 parameters[49]) are rejected. A previous study of the Pinda reservoir dolomites in Angola[30] performed in our laboratory demonstrated that dolomite samples stained with hydrocarbon could still yield high levels of contamination when cleaned through a Porapak-Q trap. The unpublished raw data from this Pinda reservoir study[30] showed that low-temperature OPA treatment solved the contamination issue (Δ_{48} offset, 6.8‰–20‰; 49 parameters, 0.389–0.525; data presented in Table 3). Even in the 5 min OPA treatment, both these contamination indicators were reduced significantly to within acceptable values (Δ_{48} offset, 0.270‰–0.407‰; 49 parameters, 0.087–0.174; Table 3). Due to the low-temperature OPA treatment, the proportion of acquisitions showing an acceptable level of contamination increased to 77.8%[30] (Figure 3).

4.2 | Effect of the OPA treatment on Δ_{47}

Our results reveal that for the RF of our instruments, a 30 min OPA treatment has the potential to cause an observable systematic positive offset in clumped isotopes (Δ_{47} values). However, if the total duration of the 30 min of OPA treatment is applied in successive 10 min treatments followed by stirring, no significant increase in the Δ_{47} value is observed. This suggests that for an offset to exist, the same mineral surface needs to be exposed to the plasma for 30 min, as stirring between runs effectively exposes new crystal surfaces between each run.

Although not statistically significant in the ANOVA tests (Δ_{47} offset of 0.014‰ for IOL, 0.024‰ for JMF-6A and 0.011‰ for

TABLE 3 A result of carbonate clumped isotope parameter (Δ_{47} value) after OPA pre-treatment and the reduction of the contaminant level of the Δ_{48} offset and the 49 parameters in hydrocarbon-saturated carbonate samples from Angola

| Sample ID	n	Δ_{47} (CDES) (‰)	Δ_{47} SE (‰)	Δ_{48} offset (‰) Mean	Δ_{48} offset (‰) Max. value	49 parameter Mean	49 parameter Max. value
Untreated sample							
Buff1	7	0.582	0.010	18.5	68.8	0.389	0.712
Caco1	7	0.566	0.026	6.8	29.6	0.525	1.996
Caco2 3637	4	0.592	0.028	20.0	62.2	0.468	0.847
Caco2 3705	3	0.543	0.016	11.7	28.2	0.465	0.855
Palang	10	0.564	0.011	19.4	162.7	0.422	0.766
5 min of OPA							
Buff1	4	0.552	0.022	0.407	0.781	0.127	0.388
Caco1	4	0.526	0.019	0.319	0.424	0.087	0.108
Caco2 3637	4	0.581	0.016	0.227	0.510	0.174	0.289
Caco2 3705	4	0.553	0.021	0.107	0.270	0.086	0.122
Palang	3	0.535	0.008	0.393	0.480	0.151	0.188

The data set is obtained from the unpublished data measured by MacDonald et al.[30]
CDES, carbon dioxide equilibrated scale; OPA, oxygen plasma ashing.

ICM), all the 30 min non-stop OPA treatments consistently yielded a different population of results, with a positive offset from the control population, as is numerically proven by the multiple comparison test LSD. It is interesting to note that the same treatment for ICM yielded the smallest Δ_{47} alteration. We suggest two possible hypotheses to explain this: either (hypothesis 1) the increase in Δ_{47} is proportional to the initial Δ_{47} value of the material as ICM has the lowest initial Δ_{47} value of the three samples, or (hypothesis 2) the effect of OPA treatment is proportional to differences in mineral reactivity given that only ICM was impacted by metamorphic processes.

The easiest explanation for a change in Δ_{47} proportional to the initial value of the sample (hypothesis 1) is admixing of a newly formed calcite mineral during OPA treatment. One of the by-products of OPA treatment is water vapour inside the plasma chamber, which has the potential to lead to isotopic exchange between the calcite and water molecule via dissolution–precipitation processes. If this was the case, the isotopic exchange would probably occur at the outer surface of the calcite mineral and would yield a new composition for the newly formed calcite with a Δ_{47} value in equilibrium with the plasma chamber

temperature of 65°C–70°C, that is, 0.577‰–0.588‰.[49] This newly precipitated calcite phase would mix with the existing samples, and we might thus expect to see an increase in the Δ_{47} final value for ICM because the initial Δ_{47} values of this sample are lower than the chamber temperature and also a lowering of the Δ_{47} value for both IOL and JMF-6A. This predicted trend is incompatible with our results for IOL and JMF-6A, and thus hypothesis 1 is rejected.

A difference in mineral reactivity (hypothesis 2) could, for instance, impact the parameters of solid-state reordering.[3] However, the low temperature recorded in the plasma chamber (<100°C) effectively precludes this process from happening. Other potential mineral reactivity mechanisms to explain how OPA treatment impacts clumped isotopes include, for instance, thermal dilatation. It is known that thermal dilatation or expansion of calcite minerals may occur in the powdered samples during the plasma treatment: a heating/cooling cycle of +20°C, −60°C, −20°C on Italian marble resulted in thermal expansion leading to a reduction in the cohesion strength of the grains.[66] The volumetric thermal expansion of limestones is also 14.5% larger[67] than that of marbles for the temperature range of 20°C–100°C; as a consequence, the thermal

FIGURE 3 Oxygen plasma ashing pre-treatment rate of success on carbonate reservoir samples contaminated by hydrocarbon (bitumen), based on 57 carbonate clumped isotope measurement of MacDonald et al.[30] The clumped isotope measurement rate of success based on acceptance of Δ_{48} offset and 49 parameter contaminant level [Color figure can be viewed at wileyonlinelibrary.com]
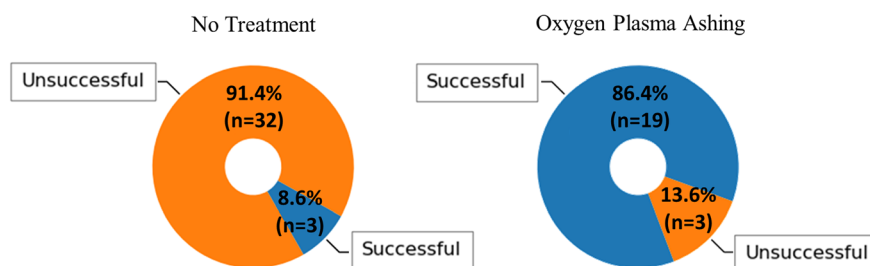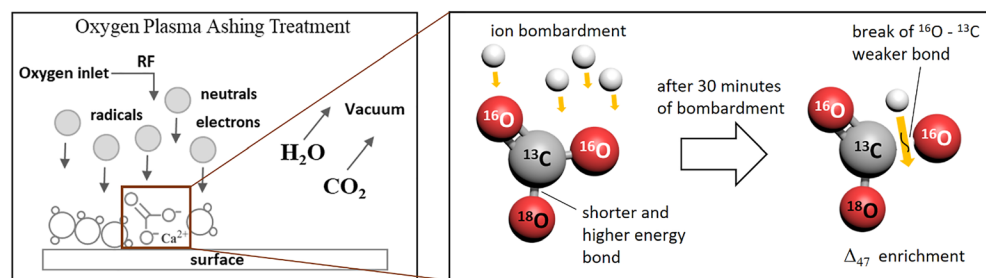
FIGURE 4 Hypothetical model for Δ_{47} enrichment by preferential breaking of the weaker bonds (e.g., $^{13}C-^{16}O$) after 30 min of oxygen plasma ashing treatment [Color figure can be viewed at wileyonlinelibrary.com]

TABLE 4 Temperature difference comparison of untreated samples and the 30 min treatment

Sample ID	Δ_{47} (‰, CDES)		Temperature, $T_{\Delta47}$ (°C)		Temperature difference (°C)
	Untreated	After 30 min OPA	Untreated	After 30 min OPA	
IOL/Oamaru limestone, New Zealand	0.732	0.746	12.7	8.8	3.9
JMF-6A/Jabal Madar calcite vein, Oman	0.629	0.653	47.2	38.1	9.1
ICM/Carrara marble standard	0.411	0.422	199.9	186.7	13.3

CDES, carbon dioxide equilibrated scale; ICM, internal Carrara marble; IOL, internal Oamaru limestone; JMF-6A, Jabal Madar.

expansion of IOL and JMF-6A would yield a larger mineral surface area to the plasma bombardment than for the ICM sample. Previous documented experiment[33] suggested that a larger surface area of calcite exposed to the plasma tends to increase the potential for atmospheric CO_2 isotopic exchange reaction due to disruption on the calcite lattice. Therefore, we suggest that the smaller Δ_{47} offset between ICM and the two other samples for the 30 min OPA treatment could be due to the different volumetric thermal expansion properties, with marbles (ICM) being less susceptible to thermal expansion. This smaller offset could also be related to data size, as the SE of the 30 min OPA of ICM is wider than that of other samples. However, if the thermal expansion hypothesis can explain the difference in magnitude of the impact of the OPA treatment in the three samples, it cannot explain why the Δ_{47} value is increasing in the 30 min treatment in the first place.

Careful observations of the petri dish after 30 min of plasma treatment revealed the occurrence of highly adhesive white particles (potentially CaO, although this could not be tested) on the side of the petri dish, suggesting that high-energy reactive species in the plasma treatment were able to sputter a small amount of carbonate material over the entire petri dish surface. Such a high-energy bombardment is likely not only to project particles out of the petri dish but also to break organic and inorganic carbon bonds at the surface of the calcite particles. As the Δ_{47} measurement depends on the relative abundance of $^{13}C-^{18}O$ bonds, and as the bond containing the heavy isotope is slightly stronger,[68] we postulate that the increasing value of Δ_{47} after the 30 min plasma experiment is due to the preferential breaking of the bonds between the lighter isotopes caused by the high-energy reactive species in the plasma. This process would lead to a progressive increase in the proportion of $^{13}C-^{18}O$ bonds at the surface of the calcite minerals, and thus an increase in Δ_{47} (Figure 4).

4.3 | Implications for paleotemperature reconstructions

As Δ_{47} has a quantitative relationship with temperature, the implications of the observed offset caused by OPA treatment can be quantified using the following temperature calibration[49]:

$$\Delta_{47} = 0.03998 \frac{10^6}{T^2} + 0.2423.$$

The difference between the initial temperature of the sample and the temperature after 30 min of continuous oxygen plasma treatment induces a bias towards a colder temperature of 3.9°C for IOL, 9.1°C for JMF-6A and 13.3°C for ICM (Table 4). Whether this bias is significant will depend on the particular application. In paleoclimate studies, the order of magnitude of change in Δ_{47} for 30 min corresponds to a large enough temperature difference to potentially mask the paleoclimatic signal investigated. However, we also note again that shorter OPA treatments of 10 min do not significantly alter the Δ_{47} value and can thus be considered safe for clumped isotope applications.

5 | CONCLUSIONS

An effective treatment to remove organic material before the carbonate clumped isotope analysis must maintain the original isotopic composition of the mineral while removing contaminants. Based on our data, 30 min or more of OPA on calcite powders has the potential to alter the initial isotopic composition beyond the analytical error, thus biasing paleotemperature studies. The small data populations used for the test prevented us from proving the statistical significance (α = 0.05) of the OPA alteration.

We postulate that this positive offset occurs because the bonds between the lighter isotopes are preferentially broken by OPA treatment, leading to an increase in the 'clumping' of the sample. Because the magnitude of the observed mean value can range from 4°C to 13°C in the 30 min treatment, we recommend that any laboratory performing OPA should reduce the runs to 10–20 min, as the plasma treatment of this duration on our instrument shows no alteration of the initial value of Δ_{47}. In addition, it is possible to safely remove additional organic matter by performing successive runs of 10 min followed by a break and stirring of the sample, as this procedure with a total OPA time of 30 min, and 60 min on Carrara marble, shows no offset in the Δ_{47} value. Our results thus validate the use of OPA for clumped isotope applications and will allow future research using clumped isotopes in challenging samples, such as oil-stained carbonates, bituminous shales and very high organic carbon content host rocks. Future research should consider the potential OPA effects on different minerals (eg, aragonite).

ACKNOWLEDGEMENTS

ORCID

Qi Adlan https://orcid.org/0000-0002-4571-9903
Cédric M. John https://orcid.org/0000-0001-9711-1548

REFERENCES

1. Ghosh P, Eiler J, Campana SE, Feeney RF. Calibration of the carbonate 'clumped isotope' paleothermometer for otoliths. *Geochim Cosmochim Acta*. 2007;71(11):2736-2744.
2. Dennis KJ, Schrag DP. Clumped isotope thermometry of carbonatites as an indicator of diagenetic alteration. *Geochim Cosmochim Acta*. 2010;74(14):4110-4122.
3. Passey BH, Henkes GA. Carbonate clumped isotope bond reordering and geospeedometry. *Earth Planet Sci Lett*. 2012;351:223-236.
4. Henkes GA, Passey BH, Grossman EL, Shenton BJ, Perez-Huerta A, Yancey TE. Temperature limits for preservation of primary calcite clumped isotope paleotemperatures. *Geochim Cosmochim Acta*. 2014; 139:362-382.
5. Huntington KW, Lechler AR. Carbonate clumped isotope thermometry in continental tectonics. *Tectonophysics*. 2015;647: 1-20.
6. Shenton BJ, Grossman EL, Passey BH, et al. Clumped isotope thermometry in deeply buried sedimentary carbonates: The effects of bond reordering and recrystallization. *Geol Soc Am Bull*. 2015; 127(7-8):1036-1051.
7. Gallagher TM, Sheldon ND, Mauk JL, Petersen SV, Gueneli N, Brocks JJ. Constraining the thermal history of the north American midcontinent rift system using carbonate clumped isotopes and organic thermal maturity indices. *Precambrian Res*. 2017;294:53-66.
8. Ryb U, Lloyd MK, Stolper DA, Eiler JM. The clumped-isotope geochemistry of exhumed marbles from Naxos, Greece. *Earth Planet Sci Lett*. 2017;470:1-12.

9. John CM. Burial estimates constrained by clumped isotope thermometry: Example of the lower cretaceous Qishn formation (Haushi-Huqf high, Oman). *Geol Soc Lond Spec Publ*. 2018;435: 107-121.
10. Mangenot X, Gasparrini M, Rouchon V, Bonifacie M. Basin-scale thermal and fluid flow histories revealed by carbonate clumped isotopes (Δ_{47}) - middle Jurassic carbonates of the Paris Basin depocentre. *Sedimentology*. 2018;65(1):123-150.
11. Huntington KW, Budd DA, Wernicke BP, Eiler JM. Use of clumped-isotope thermometry to constrain the crystallization temperature of diagenetic calcite. *J Sediment Res*. 2011;81(9-10):656-669.
12. Loyd SJ, Corsetti FA, Eiler JM, Tripati AK. Determining the diagenetic conditions of concretion formation: Assessing temperatures and pore waters using clumped isotopes. *J Sediment Res*. 2012;82(11-12): 1006-1016.
13. Dale A, John CM, Mozley PS, Smalley PC, Muggeridge AH. Time-capsule concretions: Unlocking burial diagenetic processes in the Mancos shale using carbonate clumped isotopes. *Earth Planet Sci Lett*. 2014;394:30-37.
14. Millan MI, Machel HG, Bernasconi SM. Constraining temperatures of formation and composition of dolomitizing fluids in the upper Devonian Nisku formation (Alberta, Canada) with clumped isotopes. *J Sediment Res*. 2016;86(2):107-112.
15. Ferry JM, Passey BH, Vasconcelos C, Eiler JM. Formation of dolomite at 40-80 degrees C in the Latemar carbonate buildup, Dolomites, Italy, from clumped isotope thermometry. *Geology*. 2011;39(6): 571-574.
16. Beckert J, Vandeginste V, John CM. Relationship between karstification and burial dolomitization in Permian platform carbonates (lower Khuff — Oman). *Sediment Geol*. 2016;342: 165-179.
17. Veillard CMA, John CM, Krevor S, Najorka J. Rock-buffered recrystallization of Marion plateau dolomites at low temperature evidenced by clumped isotope thermometry and X-ray diffraction analysis. *Geochim Cosmochim Acta*. 2019;252:190-212.
18. Lukoczki G, Haas J, Gregg JM, Machel HG, Kele S, John CM. Multi-phase dolomitization and recrystallization of middle Triassic shallow marine–peritidal carbonates from the Mecsek Mts. (SW Hungary), as inferred from petrography, carbon, oxygen, strontium and clumped isotope data. *Mar Pet Geol*. 2019;101:440-458.
19. Budd DA, Frost EL, Huntington KW, Allwardt PF. Syndepositional deformation features in high-relief carbonate platforms: Long-lived conduits for diagenetic fluids. *J Sediment Res*. 2013;83(1-2):14-38.
20. Lu YC, Song SR, Taguchi S, et al. Evolution of hot fluids in the Chingshui geothermal field inferred from crystal morphology and geochemical vein data. *Geothermics*. 2018;74:305-318.
21. Lu YC, Song SR, Wang PL, et al. Magmatic-like fluid source of the Chingshui geothermal field, NE Taiwan evidenced by carbonate clumped-isotope paleothermometry. *J Asian Earth Sci*. 2017;149: 124-133.
22. Honlet R, Gasparrini M, Muchez P, Swennen R, John CM. A new approach to geobarometry by combining fluid inclusion and clumped isotope thermometry in hydrothermal carbonates. *Terra Nova*. 2018; 30(3):199-206.
23. Affek HP, Bar-Matthews M, Ayalon A, Matthews A, Eiler JM. Glacial/interglacial temperature variations in Soreq cave speleothems as recorded by 'clumped isotope' thermometry. *Geochim Cosmochim Acta*. 2008;72(22):5351-5360.
24. Meckler AN, Affolter S, Dublyansky YV, et al. Glacial–interglacial temperature change in the tropical West Pacific: A comparison of stalagmite-based paleo-thermometers. *Quaternary Sci Rev*. 2015;127: 90-116.
25. Huntington KW, Wernicke BP, Eiler JM. Influence of climate change and uplift on Colorado plateau paleotemperatures from carbonate

clumped isotope thermometry. *Tectonics*. 2010;29(3):TC3005. https://doi.org/10.1029/2009TC002449

26. Swanson EM, Wernicke BP, Eiler JM, Losh S. Temperatures and fluids on faults based on carbonate clumped-isotope thermometry. *Am J Sci*. 2012;312(1):1-21.

27. Mering JA, Barker SLL, Huntington KW, et al. Taking the temperature of hydrothermal ore deposits using clumped isotope thermometry. *Econ Geol*. 2018;113(8):1671-1678.

28. del Real PG, Maher K, Kluge T, Bird DK, Brown GE, John CM. Clumped-isotope thermometry of magnesium carbonates in ultramafic rocks. *Geochim Cosmochim Acta*. 2016;193:222-250.

29. Vandeginste V, John CM, Cosgrove JW, Manning C. Dimensions, texture-distribution, and geochemical heterogeneities of fracture-related dolomite geobodies hosted in Ediacaran limestones, northern Oman. *Aapg Bull*. 2014;98(9):1789-1809.

30. MacDonald J, John C, Girard JP. Dolomitization processes in hydrocarbon reservoirs: Insight from geothermometry using clumped isotopes. *Proc Earth Plan Sci*. 2015;13:265-268.

31. Davies AJ, John CM. Reducing contamination parameters for clumped isotope analysis: The effect of lowering Porapak™ Q trap temperature to below -50 degrees C. *Rapid Commun Mass Spectrom*. 2017;31(16):1313-1323.

32. Wierzbowski H. Effects of pre-treatments and organic matter on oxygen and carbon isotope analyses of skeletal and inorganic calcium carbonate. *Int J Mass Spectrom*. 2007;268(1):16-29.

33. Roberts LR, Holmes JA, Leng MJ, Sloane HJ, Horne DJ. Effects of cleaning methods upon preservation of stable isotopes and trace elements in shells of Cyprideis torosa (Crustacea, Ostracoda): Implications for palaeoenvironmental reconstruction. *Quaternary Sci Rev*. 2018;189:197-209.

34. Fallet U, Boer W, van Assen C, Greaves M, Brummer G-JA. A novel application of wet oxidation to retrieve carbonates from large organic-rich samples for ocean-climate research. *Geochem Geophys Geosyst*. 2009;10(8):Q08004. https://doi.org/10.1029/2009GC002573

35. Huntington KW, Eiler JM, Affek HP, et al. Methods and limitations of 'clumped' CO_2 isotope (Δ_{47}) analysis by gas-source isotope ratio mass spectrometry. *J Mass Spectrom*. 2009;44(9):1318-1329.

36. Eiler JM, Schauble E. 18O13C16O in Earth's atmosphere. *Geochim Cosmochim Acta*. 2004;68(23):4767-4777.

37. Boomer I. Paleoenvironmental indicators from Late Holocene and contemporary Ostracoda of the Aral Sea. *Palaeogeogr Palaeocl*. 1993;103(3-4):141-153.

38. Lebeau O, Busigny V, Chaduteau C, Ader M. Organic matter removal for the analysis of carbon and oxygen isotope compositions of siderite. *Chem Geol*. 2014;372:54-61.

39. Epstein S, Buchsbaum R, Lowenstan HA, Urey HC. Revised carbonate-water isotopic temperature scale. *GSA Bull*. 1953;64(11):1315-1326.

40. Epstein S, Buchsbaum R, Lowenstam H, Urey HC. Carbonate-water isotopic temperature scale. *GSA Bull*. 1951;62(4):417-426.

41. Curtis JH, Hodell DA. An isotopic and trace element study of ostracods from Lake Miragoane, Haiti: A 10,500 year record of paleosalinity and paleotemperature changes in the Caribbean. In: Swart PK, Lohmann KC, McKenzie J, Savin S, eds. *Climate Change in Continental Isotopic Records*. Geophysical Monograph Series Vol. 78. Washington, DC: American Geophysical Union; 1993:135-152.

42. Durazzi JT. Stable isotopes in ostracod shell - preliminary-study. *Geochim Cosmochim Acta*. 1977;41(8):1168-1170.

43. Lister GS. A 15,000-year isotopic record from Lake Zürich of deglaciation and climatic change in Switzerland. *Quatern Res*. 1988;29(2):129-141.

44. Goreau TJ, Yonge M. Coral skeletal chemistry: Physiological and environmental regulation of stable isotopes and trace metals in

Montastrea annularis. *Proc R Soc London Series B Biological Sciences*. 1977;196(1124):291-315.

45. Bird MI, Charville-Mort PDJ, Ascough PL, Wood R, Higham T, Apperley D. Assessment of oxygen plasma ashing as a pre-treatment for radiocarbon dating. *Quat Geochronol*. 2010;5(4):435-442.

46. Pike S, Dewison MG, Spears DA. Sources of error in low-temperature plasma ashing procedures for quantitative mineral analysis of coal ash. *Fuel*. 1989;68(5):664-668.

47. Nelson CS, Smith AM. Stable oxygen and carbon isotope compositional fields for skeletal and diagenetic components in New Zealand Cenozoic nontropical carbonate sediments and limestones: A synthesis and review. *New Zealand J Geol Geophys*. 1996;39(1):93-107.

48. Vandeginste V, Stehle MC, Jourdan A-L, Bradbury HJ, Manning C, Cosgrove JW. Diagenesis in salt dome roof strata: Barite - calcite assemblage in Jebel Madar, Oman. *Mar Petr Geol*. 2017;86:408-425.

49. Davies AJ, John CM. The clumped (13C18O) isotope composition of echinoid calcite: Further evidence for "vital effects" in the clumped isotope proxy. *Geochim Cosmochim Acta*. 2019;245:172-189.

50. Dai XJ. Kinetic model of an RF discharge in oxygen. *Aust J Phys*. 1996;49(6):1169-1180.

51. McCrea JM. On the isotopic chemistry of carbonates and a Paleotemperature scale. *J Chem Phys*. 1950;18(6):849-857.

52. Swart PK, Burns SJ, Leder JJ. Fractionation of the stable isotopes of oxygen and carbon in carbon-dioxide during the reaction of calcite with phosphoric-acid as a function of temperature and technique. *Chem Geol*. 1991;86(2):89-96.

53. John CM, Bowen D. Community software for challenging isotope analysis: First applications of 'Easotope' to clumped isotopes. *Rapid Commun Mass Spectrom*. 2016;30(21):2285-32300.

54. Bernasconi SM, Hu B, Wacker U, Fiebig J, Breitenbach SFM, Rutz T. Background effects on Faraday collectors in gas-source mass spectrometry and implications for clumped isotope measurements. *Rapid Commun Mass Spectrom*. 2013;27(5):603-612.

55. Dennis KJ, Affek HP, Passey BH, Schrag DP, Eiler JM. Defining an absolute reference frame for 'clumped' isotope studies of CO_2. *Geochim Cosmochim Acta*. 2011;75(22):7117-7131.

56. Muller IA, Violay MES, Storck JC, et al. Clumped isotope fractionation during phosphoric acid digestion of carbonates at 70 degrees C. *Chem Geol*. 2017;449:1-14.

57. Petersen SV, Defliese WF, Saenger C, et al. Effects of improved 17O correction on Interlaboratory agreement in clumped isotope calibrations, estimates of mineral-specific offsets, and temperature dependence of acid digestion fractionation. *Geochem Geophys Geosyst*. 2019;20(7):3495-3519.

58. Kim ST, Mucci A, Taylor BE. Phosphoric acid fractionation factors for calcite and aragonite between 25 and 75 degrees C: Revisited. *Chem Geol*. 2007;246(3-4):135-146.

59. Guo W, Eiler JM. Temperatures of aqueous alteration and evidence for methane generation on the parent bodies of the CM chondrites. *Geochim Cosmochim Acta*. 2007;71(22):5565-5575.

60. Cohen J. The concepts of power analysis. In: Cohen J, ed. *Statistical Power Analysis for the Behavioral Sciences*. New York: Academic Press; 1977 :1-17.

61. Fisher RA. Design of experiments. *Br Med J*. 1936;1(3923):554-554.

62. Hsu JC. *Multiple Comparisons: Theory and Methods*. London: Chapman & Hall; 1996:177.

63. Petersen SV, Winkelstern IZ, Lohmann KC, Meyer KW. The effects of Porapak™ trap temperature on delta O-18, delta C-13, and delta(47) values in preparing samples for clumped isotope analysis. *Rapid Commun Mass Spectrom*. 2016;30(1):199-208.

64. Mahapoonyanont N, Mahapoonyanont T, Pengkaew N, Kamhangkit R. Power of the test of one-way Anova after

transforming with large sample size data. *Procedia Soc Behav Sci*. 2010;9:933-937.

65. Belkind A, Gershman S. Plasma cleaning of surfaces. *Vacuum Coating Technol*. 2008;November:46-57.

66. Koch A, Siegesmund S. The combined effect of moisture and temperature on the anomalous expansion behaviour of marble. *Environ Geol*. 2004;46(3-4):350-363.

67. Robertson EC. Thermal properties of rocks. U.S. Geological Survey. USGS Numbered Series; 1988. Report No.: 88-441.

68. Eiler JM. "Clumped-isotope" geochemistry - the study of naturally-occurring, multiply-substituted isotopologues. *Earth Planet Sci Lett*. 2007;262(3-4):309-327.

SUPPORTING INFORMATION

Additional supporting information may be found online in the Supporting Information section at the end of this article.